geoconvention Virtual Event September 21-23 2020
CSPG • CSEG • CWLS • GAC • MAC • IAH

Microseismic Event Location and Quality Control Workflow for Deviated Borehole

Amna Feroz[1] and Mirko van der Baan[1]
[1]University of Alberta

Summary

Detailed microseismic interpretation is based on the located microseismic events, thus these locations should be as accurate as possible. In order to have confidence in simulated rock volume calculation, it is important to understand the origin of position uncertainty in microseismic event locations. Uncertainties in microseismic event location arise due to several factors, including inaccurate velocity model, random errors associated with P and S wave arrival time picking and receiver configuration. Therefore, a good understanding of these parameters and processing workflow is required. In this chapter we propose, apply and emphasize the need for a complete processing and quality control workflow for microseismic data recorded by single monitoring well.

Introduction

Microseismic monitoring provides an insight into induced and naturally occurring stress changes during the mining operation, hydraulic fracturing, reservoir monitoring and carbon sequestration (Jones et al. 2010). The very first and most critical step in any microseismic monitoring survey is to accurately locate microseismic event locations both in time and space, thus allowing the mapping of fault and fracture network (Castellanos and van der Baan 2012; De Meersman, Kendall, and Van der Baan 2009). Once accurate event locations are determined then a detailed analysis may be performed to understand and image the reservoir.

Here in this chapter, we describe a complete workflow including the processing of microseismic data and quality control of resulted event locations. We initially remove 180^{o} degree azimuthal uncertainty by incorporating the spatial distribution of geophones placed in the deviated borehole and later invert for the hypocenter location incorporating S-P wave arrival times in a grid search manner. Next, we incorporate a combination of some of the commonly used simple but effective strategies to quality check the results. We then apply the complete workflow to a data set recorded during steam injection over a period of 4 years (2002-2005).

Event Location Workflow-Theory

Figure 1 summarizes the complete microseismic event location workflow implemented in this study. The processes can be broadly divided into six steps: 1) Data Pre-processing, 2) Arrival time picking, 3) P-wave polarization analysis, 4) Removal of 180^{o} uncertainty in azimuthal measurements, 5) Event location and 6) Quality control of the event locations.

Step 1: Data Pre-processing

First, a correction is applied to account for well inclination with the help of a well deviation survey. Next, the true position of horizontal components (h1 and h2) is determined by calculating the true azimuth of P wave polarization relative to the north using a perforation shot (with known source position often called calibration shot). This is usually repeated for all the calibration shots and the average rotation angle is calculated. The trace data is rotated such as that h1-component is parallel to the East and h2 component is parallel to the North. Raw data is mean corrected to remove any DC component; this is achieved by subtracting the data mean value from the data. Then data is then filtered to reduce the noise, a bandpass filter is normally applied.

Step2: Arrival time picking

Accurate phase picks are necessary for correct event location as errors in arrival time picks have been identified as the major factor controlling the errors in resulting microseismic event locations (Pavlis 1986). The most commonly used procedure is that of Earl and Shearer (1994), this method compares the short-term average and long-term average of the signal. However, the method is inconsistence in placing the pick on waveform e.g. first break or peak and trough.

Step 3: P wave polarization analysis - Covariance method

The P-wave azimuth is estimated using a covariance analysis of three-component data at each station. The method uses the auto and cross-variance of three-component data recorded by geophones.

Step 4: Azimuth analysis-removal of 180^{O} ambiguity

The resulting azimuthal values from covariance analysis have a 180^{o} degree ambiguity which must be resolved before inverting for event location. We may take advantage of the limited spatial spread of geophone placed in a deviated or horizontal borehole. The azimuth calculated at each receiver location is used to resolve the ambiguity. The calculated azimuths are plotted as straight ray paths at each receiver location and extended in both directions, until they converge, thus indicating the correct side of the well where the event occurred. Azimuth information of at least two stations is required to remove 180^{o} degree ambiguity. Figure 2 shows an illustration of the method.

Step 5: Event location

The fifth stage of our workflow is the location of microseismic events. In our workflow, we used a popular method, known as 'grid search' to invert for absolute event locations (Lomax, Michelini, and Curtis 2009). The procedure consists of generating a grid with nodes associated with possible hypocenter. Next, theoretical P-, S-wave arrival times and P wave azimuth are calculated for each node and compared with observed times. This will yield a likelihood estimate at each node and a grid node with max probability estimate is selected as a possible source location.

Step 6: Quality Control

The quality control procedure comprises of two parts. In the first part, each event is analyzed independent of the rest of the data. We start by comparing the observed and theoretical arrival time picks by overlaying them on the waveform. This simple step will instantly show if:

1) Observed and theoretical picks are in good agreement,
2) Observed picks have systematic and/or aleatoric errors and need to be re-picked and
3) Constant shifts occur between predicted and observed arrival times (possibly due to wrong origin time estimation) or
4) Possibly a wrong phase has been picked.

The second part involves an analysis of all event locations at once. This is done by first plotting the original and improved event locations and histogram of azimuth and S-P wave residuals. The last and another important step is to analyze the similarity between events by calculating the P-wave cross-correlation coefficient (Castellanos and van der Baan 2013). **.**

Application to Real data- Results

The data consisted of ~9,000 files, out of which 2271 files were extracted as possible events manually. The workflow was applied to the selected 2271 events and 1225 events successfully passed the quality workflow. Whereas, 1046 events were revisited and re-located (Table1). The inclusion of the dip analysis step appears to improve confidence in the event location. The revision of selected evens not only improved the individual event locations, but it is evident from that the workflow removed the scattering and improved the clustering of events around the true event location. The time residual plot of initial and final event locations may initially look the same but careful attention to the shape and size of the histogram reveals the differences. Note the difference in the shape of the histogram e.g. the residual histogram of initial event locations is skewed to the left whereas the histogram of final locations appears to be more symmetrical and a higher peak at the center (zero). The cross-correlation coefficient as a function of separation distance for final event locations shows an inverse relationship with the exception of very few outliers.

Conclusion

Locating microseismic events using a single deviated array of geophones in a 1D velocity model requires the use of P- and S-wave arrival times and azimuth information to accurately locate the events. We have developed and applied a complete workflow to process, enhance and quality control the results. Data from the cyclic steam simulation experiment is used to test the complete processing and quality control workflow. First, we make use of the deviated geometry to resolve the 180^{o} uncertainty associated with azimuth and then use S-P wave time difference and azimuth to constrain the event location. This is followed by step by step approach to quality control the microseismic event locations by using commonly used techniques. The workflow once applied, improved the results and highlighted the common sources of errors that result in event location uncertainty.

Acknowledgments

We sincerely thank the sponsors of the Microseismic Industry Consortium for supporting this research, and an anonymous company for providing the data and permission to show the results.

References

Reference Style (use Arial 9pt normal)

Allen, Rex V. 1978. "Automatic Earthquake Recognition and Timing from Single Traces." *Bulletin of the Seismological Society of America* 68(5): 1521–32.

Baer, M, and U Kradolfer. 1987. "An Automatic Phase Picker for Local and Teleseismic Events." *Bulletin of the Seismological Society of America* 77(4): 1437–45.

Castellanos, Fernando, and Mirko van der Baan. 2012. "High-Accuracy Relative Event Locations Using a Combined Multiplet Analysis and the Double-Difference Inversion." In *SEG Technical Program Expanded Abstracts 2012*, Society of Exploration Geophysicists, 1–5.

Castellanos, Fernando, and Mirko van der Baan. 2013. "Microseismic Event Locations Using the Double-Difference Algorithm." *CSEG Recorder* 38(3): 26–37.

Geiger, Ludwig. 1912. "Probability Method for the Determination of Earthquake Epicenters from the Arrival Time Only." *Bull. St. Louis Univ* 8(1): 56–71.

Gentili, Stefania, and Alberto Michelini. 2006. "Automatic Picking of P and S Phases Using a Neural Tree." *Journal of Seismology* 10(1): 39–63.

Jones, G A, J-M Kendall, I D Bastow, and D G Raymer. 2013. "Locating Microseismic Events Using Borehole Data." *Geophysical Prospecting* 62(1): 34–49.

Jones, G A, D Raymer, K Chambers, and J-M Kendall. 2010. "Improved Microseismic Event Location by Inclusion of a Priori Dip Particle Motion: A Case Study from Ekofisk." *Geophysical prospecting* 58(5): 727–37.

Lomax, Anthony, Alberto Michelini, and Andrew Curtis. 2009. "Earthquake Location, Direct, Global-Search Methods." *Encyclopedia of complexity and systems science*: 2449–73.

De Meersman, K, J-M Kendall, and M Van der Baan. 2009. "The 1998 Valhall Microseismic Data Set: An Integrated Study of Relocated Sources, Seismic Multiplets, and S-Wave Splitting." *Geophysics* 74(5): B183–95.

Pavlis, Gary L. 1986. "Appraising Earthquake Hypocenter Location Errors: A Complete, Practical Approach for Single-Event Locations." *Bulletin of the Seismological Society of America* 76(6): 1699–1717.

Rentsch, S, S Buske, S Lüth, and A Shapiro. 2006. "Fast Location of Seismicity: A Migration-Type Approach with Application to Hydraulic-Fracturing Data." *Geophysics* 72(1): S33–40.

Rodi, William. 2006. "Grid-Search Event Location with Non-Gaussian Error Models." *Physics of the Earth and Planetary Interiors* 158(1): 55–66.

Sleeman, Reinoud, and Torild Van Eck. 1999. "Robust Automatic P-Phase Picking: An on-Line Implementation in the Analysis of Broadband Seismogram Recordings." *Physics of the earth and planetary interiors* 113(1–4): 265–75.

Zhou, Rongmao, Lianjie Huang, and James Rutledge. 2010. "Microseismic Event Location for Monitoring CO 2 Injection Using Double-Difference Tomography." *The Leading Edge* 29(2): 208–14.

Zhou, Wen et al. 2015. "Microseismic Event Location Using an Inverse Method of Joint P–S Phase Arrival Difference and P-Wave Arrival Difference in a Borehole System." *Journal of Geophysics and Engineering* 12(2): 220–26.

Data Summary

Event Count	Comments

Total no. of Events	2271	Microseismic events recorded from 2002 to 2005.
QC passed Events	1225	Events located and passed the quality check.
Revisited Events	1046	Arrival times were revisited, azimuth re-calculated and events relocated.
Disabled Events	~190	Limited no of picks, very noisy data

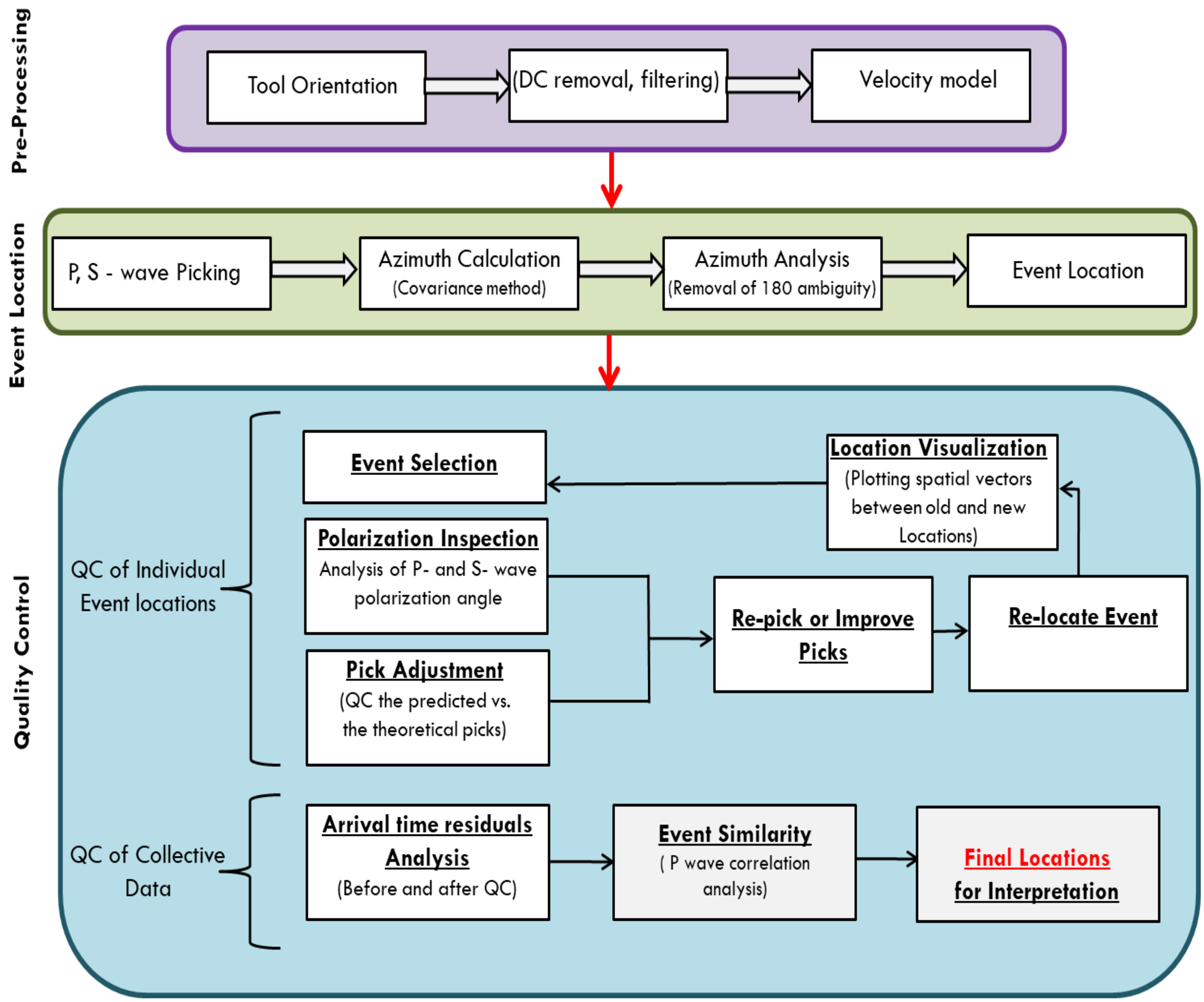

Figure1: Flowchart diagram illustrating the complete Microseismic processing workflow employed in this study.

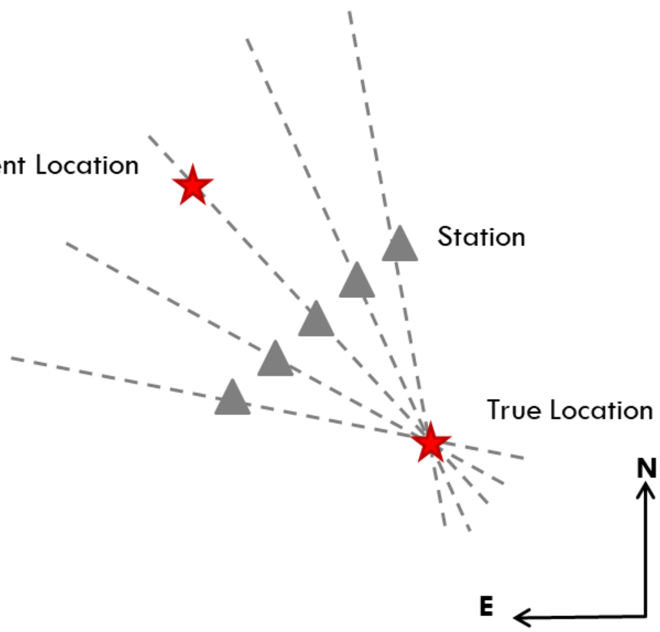

Figure 2. Illustration of the azimuth analysis, the dashed line represents the P –wave particle motion/ray path, a red star represents the microseismic source location and grey triangles are the geophones.